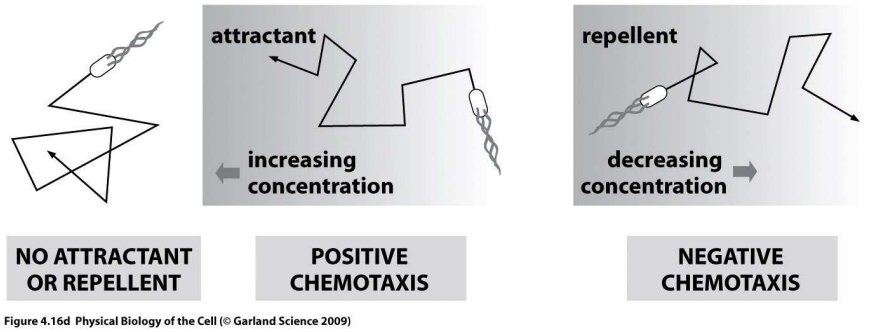

Figure 5.5: Examples of chemotaxis. Figure from Phillips, Kondev and Theriot [34]; used with permission of Garland Science.

5.4 Bacterial Chemotaxis

Chemotaxis refers to the process by which micro-organisms move in response to chemical stimuli. Examples of chemotaxis include the ability of organisms to move in the direction of nutrients or move away from toxins in the environment. Chemotaxis is called *positive chemotaxis* if the motion is in the direction of the stimulus and *negative chemotaxis* if the motion is away from the stimulant, as shown in Figure 5.5. Many chemotaxis mechanisms are stochastic in nature, with biased random motions causing the average behavior to be either positive, negative or neutral (in the absence of stimuli).

In this section we look in some detail at bacterial chemotaxis, which *E. coli* use to move in the direction of increasing nutrients. The material in this section is based primarily on the work of Barkai and Leibler [8] and Rao, Kirby and Arkin [36].

Control system overview

The chemotaxis system in *E. coli* consists of a sensing system that detects the presence of nutrients, and actuation system that propels the organims in its environment, and control circuitry that determines how the cell should move in the presence of chemicals that stimulate the sensing system. The approximate location of these elements are shown in Figure **??**.

The actuation system in the *E. coli* consists of a set of flagella that can be spun using a flagellar motor embedded in the outer membrane of the cell, as shown in Figure 5.6a. When the flagella all spin in the counter clockwise direction, the individual flagella form a bundle and cause the organism to move roughly in a straight line. This behavior if called a "run" motion. Alternatively, if the flagella spin in the clockwise direction, the individual flagella do not form a bundle and the organism "tumbles", causing it to rotate (Figure 5.6b). The selection of the motor direction is controlled by the protein CheY: if phosphorylated CheY binds to the

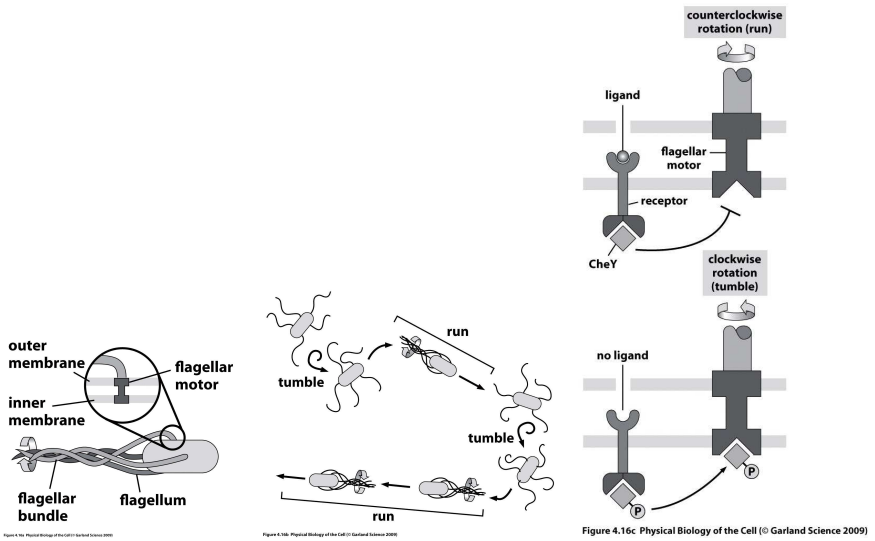

(a) (b) (c)

Figure 5.6: Bacterial chemotaxis. Figures from Phillips, Kondev and Theriot [34]; used with permission of Garland Science.

motor complex, the motor spins clockwise (tumble), otherwise it spins counter-clockwise (run).

Because of the size of the organism, it is not possible for a bacterium to sense gradients across its length. Hence, a more sophisticated strategy is used, in which the organism undergoes a combination of run and tumble motions. The basic idea is illustrated in Figure 5.6c: when high concentration of ligand (nutrient) is present, the CheY protein is left unphosphorylated and does not bind to the actuation complex, resulting in a counter-clockwise rotation of the flagellar motor (run). Conversely, if the ligand is present then the molecular machinery of the cell causes CheY to be phosphorylated and this modifies the flagellar motor dynamics so that a clockwise rotation occurs (tumble). The net effect of this combination of behaviors is that when the organism is traveling through regions of higher nutrient concentration, it continues to move in a straight line for a longer period before tumbling, causing it to move in directions of increasing nutrient concentration.

A simple model for the molecular control system that regulates chemotaxis is shown in Figure 5.7. We start with the basic sensing and and actuation mechanisms. A membrane bound protein MCP (methyl-accepting chemotaxis protein) that is capable of binding to the external ligand serves as a signal transducing element from the cell exterior to the cytoplasm. Two proteins, CheW and CheA, form a complex with MCP. This complex can either be in an active or inactive state. In the active state, CheA is autophosphorylated and serves as a phosphotransferase for

RMM: Obtain permission

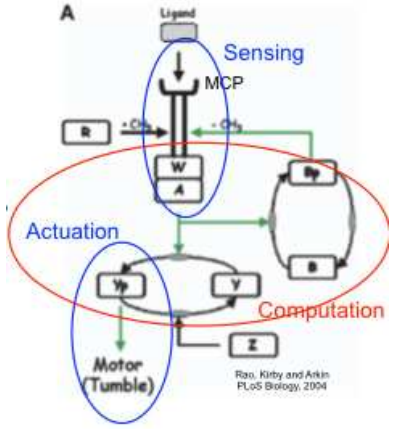

Figure 5.7: Control system for chemotaxis. Figure from Rao *et al*. [36] (Figure 1A).

two additional proteins, CheB and CheY. The phosphorylated form of CheY then binds to the motor complex, causing clockwise rotation of the motor.

The activity of the receptor complex is governed by two primary factors: the binding of a ligand molecule to the MCP protein and the presence or absence of up to 4 methyl groups on the MCP protein. The specific dependence on each of these factors is somewhat complicated. Roughly speaking, when the ligand L is bound to the receptor then the complex is less likely to be active. Furthermore, as more methyl groups are present, the ligand binding probability increases, allowing the gain of the sensor to be adjusted through methylation. Finally, even in the absence of ligand the receptor complex can be active, with the probability increasing with increased methylation. Figure 5.8 summarizes the possible states, their free energies and the probability of activity.

Several other elements are contained in the chemotaxis control circuit. The most important of these are implemented by the proteins CheR and CheB, both of which affect the receptor complex. [**?**], which is constitutively produced in the cell, methylates the receptor complex at one of the four different methylation sites. Conversely, the phosphorylated form of CheB demethylates the receptor complex. As described above, the methylation patterns of the receptor complex affect its activity, which in turn affects the phosphorylation of CheA and, in turn, phosphorylation of CheY and CheB. The combination of CheA, CheB and the methylation of the receptor complex forms a negative feedback loop: if the receptor is active, then CheA phosphorylates CheB, which in turn demethylates the receptor complex, making it less active. As we shall see when we investigate the detailed dynamics, this feedback loop corresponds to an integral feedback law. This integral action allows the cell to adjust to different levels of ligand concentration, so that the behavior of the system is invariant to the absolute nutrient levels (this is explained in more detail below).

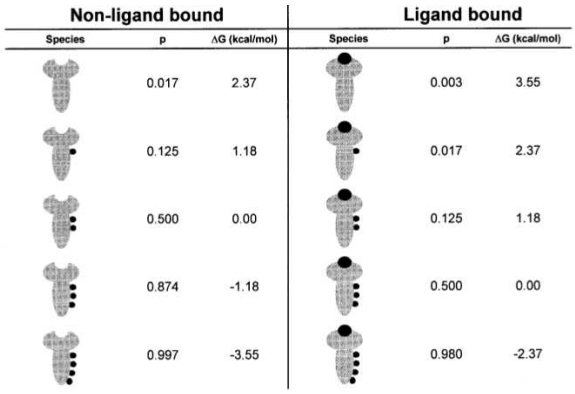

Figure 5.8: Receptor complex states. The probability of a given state being in an active configuration is given by p. Figure obtained from [**?**].

Modeling

The detailed reactions that implement chemotaxis are illustrated in Figure **??**. Letting T represent the receptor complex and T^A represent an active form, the basic reactions can be written as

$$\begin{aligned} T^A + A &\rightleftharpoons T^A{:}A \longrightarrow A^p + T^A \\ A^p + B &\rightleftharpoons A^p{:}B \longrightarrow A + B^p \qquad B^p + P \rightleftharpoons B^p{:}P \longrightarrow B + P \\ A^p + Y &\rightleftharpoons A^p{:}Y \longrightarrow A + Y^p \qquad Y^p + Z \rightleftharpoons Y^p{:}P \longrightarrow Y + P \end{aligned} \tag{5.6}$$

where CheA, CheB, CheY and CheZ are written simply as A, B, Y and Z for simplicity and P is a non-specific phosphotase. We see that these are basically three linked sets of phosphorylation and dephosphorylation reactions, with CheA serving as a phosphotransferase and P and CheZ serving as phosphotases.

The description of the methylation of the receptor complex is a bit more complicated. Each receptor complex can have multiple methyl groups attached and the activity of the receptor complex depends on both the amount of methylation and whether a ligand is attached to the receptor site. Furthermore, the binding probabilities for the receptor also depend on the methylation pattern. To capture this, we use the set of reactions that are illustrated in Figure 5.10. In this diagram, T_i^s represents a receptor that has i methylation sites filled) and ligand state s (which can be either u if unoccupied or o if occupied). We let M represent the maximum number of methylation sites ($M = 4$ for *E. coli*).

Using this notation, the transitions between the states correspond to the reactions shown in Figures 5.7 and 5.9:

$$\begin{aligned} T_i^x + B^p &\rightleftharpoons T_i^x{:}B^p \longrightarrow T_{i-1}^x + B^p && i > 0 \\ T_i^x + R &\rightleftharpoons T_i^x{:}R \longrightarrow T_{i+1}^x + R && i < M \\ T_i^u + L &\rightleftharpoons T_i^o \end{aligned}$$

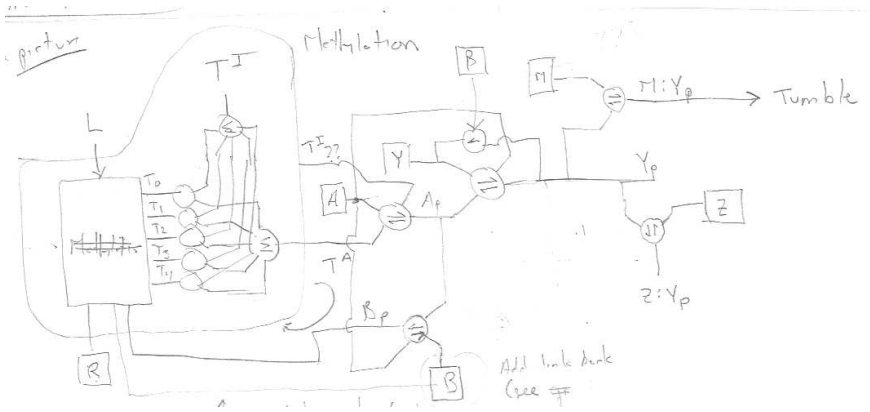

Figure 5.9: Circuit diagram for chemotaxis.

We now must write reactions for each of the receptor complexes with CheA. Each form of the receptor complex has a different activity level and so the most complete description is to write a separate reaction for each T_i^o and T_i^u species:

$$T_i^x + A \underset{k_i^{r,o}}{\overset{k_i^{f,o}}{\rightleftharpoons}} T_i^x{:}A \xrightarrow{k_i^{c,o}} A^p + T_i^x,$$

where $x \in \{o, u\}$ and $i = 0, \ldots, M$. This set of reactions replaces the placeholder reaction $T^A + A \rightleftharpoons T^A{:}A \longrightarrow A^p + T^A$ used earlier.

RMM Include simulation results on the full model here

While the equations above give a fairly complete description of the reactions that implement the chemotaxis control circuit, there are still many missing effects. Supplement

RMM Summarize some of the main features that are missing.

RMM: Obtain permission

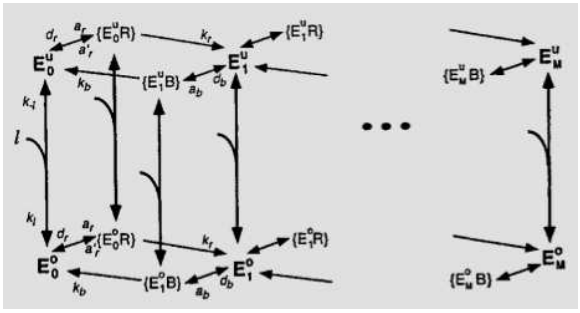

Figure 5.10: Methylation model for chemotaxis. Figure from Barkai and Leibler [8] (Box 1). Note: the figure uses the notation E_i^s for the receptor complex instead of T_i^s.

Reduced-order models

The detailed model described above is sufficiently complicated that it can be difficult to analyze. In this section we develop a slightly simpler model that can be used to explore the adaptation properties of the circuit, which happen on a slower time-scale.

We begin by simplifying the representation of the receptor complex and its methylation pattern. Let $L(t)$ represent the ligand concentration and T_i represent the concentration of the receptor complex with i sides methylated. If we assume that the binding reaction of the ligand L to the complex is fast, we can write the probability that a receptor complex with i sites methylated is in its active state as a static function $\alpha_i(L)$, which we take to be of the form

$$\alpha_i(L) = \frac{\alpha_i^o L}{K_L + L} + \frac{\alpha_i K_L}{K_L + L}.$$

The coefficients α_i^o and α_i capture the effect of presence or absence of the ligand on the activity level of the complex. Note that α_i has the form of a Michaelis-Menten function, reflecting our assumption that ligand binding is fast compared to the rest of the dynamics in the model. Following [**?**], we take the coefficients to be

$$\begin{aligned} a_0 &= 0, & a_1 &= 0.1, & a_2 &= 0.5, & a_3 &= 0.75, & a_4 &= 1, \\ a_0^o &= 0, & a_1^o &= 0, & a_2^o &= 0.1, & a_3^o &= 0.5, & a_4^o &= 1. \end{aligned}$$

and choose $K_L = 10\ \mu\text{M}$.

The total concentration of active receptors can now be written in terms of the receptor complex concentrations T_i and the activity probabilities $\alpha_i(L)$. We write the concentration of activated complex T^A and inactivated complex T^I as

$$T^A = \sum_{i=0}^{4} \alpha_i(L) T_i, \qquad T^I = \sum_{i=0}^{4} (1 - \alpha_i(L)) T_i.$$

These formulas can now be used in our dynamics as an effective concentration of active or inactive receptors, justifying the notation that we used in equation (5.6).

We next model the transition between the methylation patterns on the receptor. We assume that the rate of methylation depends on the activity of the receptor complex, with active receptors less likely to be demethylated and inactive receptors less likely to be methylated [36, **?**]. Let

$$r_B = k_B \frac{B^p}{K_B + T^A}, \qquad r_R = k_R \frac{R}{K_R + T^I},$$

represent rates of the methylation and demethylation reactions.† We choose the coefficients as

RMM: Talk more about where these come from

$$k_B = 0.5, \quad K_B = 5.5, \quad k_R = 0.255, \quad K_R = 0.251,$$

We can now write the methylation dynamics as

$$\frac{d}{dt}T_i = r_R(1-\alpha_{i+1}(L))T_{i-1} + r_B\alpha_{i+1}(L)T_{i+1} - r_R(1-\alpha_i(L))T_i - r_B\alpha_i(L)T_i,$$

where the first and second terms represent transitions into this state via methylation or demethylation of neighboring states (see Figure 5.10) and the last two terms represent transitions out of the current state by methylation and demethylation, respectively. Note that the equations for T_0 and T_4 are slightly different since the demethylation and methylation reactions are not present, respectively.

Finally, we write the dynamics of the phosphorylation and dephosphorylation reactions, and the binding of CheY$^{\mathrm{p}}$ to the motor complex. Under the assumption that the concentrations of the phosphorylated proteins is small relative to the total protein concentration, we can approximate the reaction dynamics as

$$\begin{aligned}
\frac{d}{dt}A^p &= 50T^A A - 100A^pY - 30A^pB,\\
\frac{d}{dt}Y^p &= 100A^pY - 0.1Y^p - 5[\mathrm{M}]Y^p + 19[\mathrm{M{:}Y^p}] - 30Y^p,\\
\frac{d}{dt}B^p &= 30A^pB - B^p,\\
\frac{d}{dt}[\mathrm{M{:}Y^p}] &= 5[\mathrm{M}]Y^p - 19[\mathrm{M{:}Y^p}].
\end{aligned}$$

The total concentrations of the species are given by

$$A + A^p = 5\ \mathrm{nM}, \qquad B + B^p = 2\ \mathrm{nM}, \qquad Y + Y^p + [\mathrm{M{:}Y^p}] = 17.9\ \mathrm{nM},$$
$$[\mathrm{M}] + [\mathrm{M{:}Y^p}] = 5.8\ \mathrm{nM}, \qquad R = 0.2\ \mathrm{nM}, \qquad \textstyle\sum_{i=0}^{4} T_i = 5\ \mathrm{nM}.$$

The reaction coefficients and concentrations are taken from Rao *et al* [36].

Figure 5.11a shows a the concentration of the phosphorylated proteins based on a simulation of the model. Initially, all species are started in their unphosphorylated and unmethylated states. At time $T = 500$ s the ligand concentration is increased to $L = 10$ μM and at time $T = 1000$ it is returned to zero. We see that immediately after the ligand is added, the CheY$^{\mathrm{p}}$ concentration drops, allowing longer runs between tumble motions. After a short period, however, the CheY$^{\mathrm{p}}$ concentration adapts to the higher concentration and the nominal run versus tumble behavior is restored. Similarly, after the ligand concentration is decreased the concentration of CheY$^{\mathrm{p}}$ increases, causing a larger fraction of tumbles (and subsequent changes in direction). Again, adaptation over a longer time scale returns that CheY concentration to its nominal value.

Figure 5.11b helps explain the adaptation response. We see that the average amount of methylation of the receptor proteins increases when the ligand concentration is high, which decreases the activity of CheA (and hence decreases the phosphorylation of CheY).†

RMM: Say more

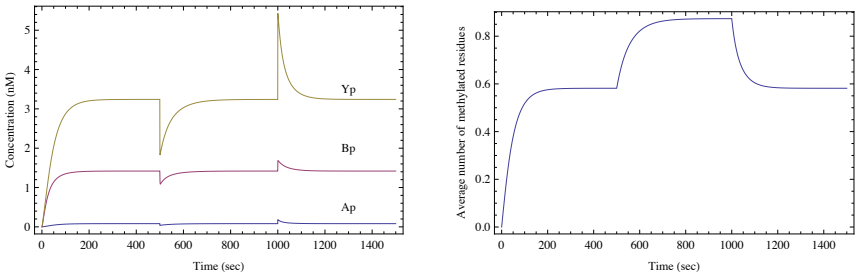

(a) (b)

Figure 5.11: Simulation and analysis of reduced-order chemotaxis model.

A simpler model can be obtained by ignoring the detailed methylation pattern completely. We can do this by modeling the entire receptor complex as a single species T that exists in an active state T^A and an inactive state T^I. We then keep track of the total methylation M, which is modulated by CheR and CheB, and use this to modulate the amount of active and inactive receptor complex, as shown in Figure 5.12. Supplement

Figure out Barkai, Leibler paper and summarize here (including simulations). **RMM**

Supplement

Integral action

The perfect adaptation mechanism in the chemotaxis control circuitry has the same function as the use of integral action in control system design: by including a feedback on the integral of the error, it is possible to provide exact cancellation to constant disturbances. In this section we demonstrate that a simplified version of the dynamics can indeed be regarding as integral action of an appropriate signal. This interpretation was first pointed out by Yi *et al* [**?**].

RMM: Obtain permission

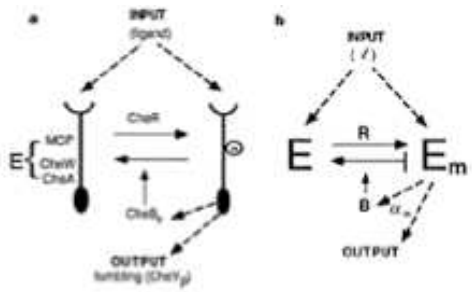

Figure 5.12: Reduced-order model for chemotaxis. Figure from Barkai and Leibler [8] (Figure 1).

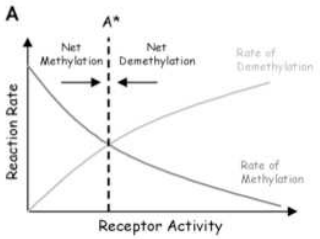

(a)

Further reading

Bibliography

[1] K. J. Åström and R. M. Murray. *Feedback Systems: An Introduction for Scientists and Engineers*. Princeton University Press, 2008. Available at http://www.cds.caltech.edu/~murray/amwiki.

[2] B. Alberts, D. Bray, J. Lewis, M. Raff, K. Roberts, and J. D. Watson. *The Molecular Biology of the Cell*. Garland Science, fifth edition edition, 2008.

[3] U. Alon. *An introduction to systems biology. Design principles of biological circuits*. Chapman-Hall, 2007.

[4] W. Arber and S. Linn. DNA modification and restriction. *Annual Review of Biochemistry*, 38:467–500, 1969.

[5] D. P. Atherton. *Nonlinear Control Engineering*. Van Nostrand, New York, 1975.

[6] M. R. Atkinson, M. A. Savageau, J. T. Meyers, and A. J. Ninfa. Development of genetic circuitry exhibiting toggle switch or oscillatory behavior in *Escherichia coli*. *Cell*, pages 597–607, 2003.

[7] D. Baker, G. Church, J. Collins, D. Endy, J. Jacobson, J. Keasling, P. Modrich, C. Smolke, and R. Weiss. ENGINEERING LIFE: Building a FAB for biology. *Scientific American*, June 2006.

[8] N Barkai and S Leibler. Robustness in simple biochemical networks. *Nature*, 387(6636):913–7, 1997.

[9] A. Becskei and L. Serrano. Engineering stability in gene networks by autoregulation. *Nature*, 405:590–593, 2000.

[10] F. D. Bushman and M. Ptashne. Activation of transcription by the bacteriophage 434 repressor. *PNAS*, pages 9353–9357, 1986.

[11] A. J. Courey. *Mechanisms in Transcriptional Regulation*. Wiley-Blackwell, 2008.

[12] H. de Jong†. Modeling and simulation of genetic regulatory systems: A literature review. *Journal of Computational Biology*, 9:67–103, 2002.

[13] D. Del Vecchio, A. J. Ninfa, and E. D. Sontag. Modular cell biology: Retroactivity and insulation. *Nature/EMBO Molecular Systems Biology*, 4:161, 2008.

[14] M. B. Elowitz and S. Leibler. A synthetic oscillatory network of transcriptional regulators. *Nature*, 403(6767):335–338, 2000.

[15] D. Endy. Foundations for engineering biology. *Nature*, 438:449–452, 2005.

[16] T.S. Gardner, C.R. Cantor, and J.J. Collins. Construction of the genetic toggle switch in *Escherichia Coli*. *Nature*, page 339342, 2000.

RMM: Check alphabetical order

[17] D. T. Gillespie. *Markov Processes: An Introduction For Physical Scientists*. Academic Press, 1976.

[18] D. T. Gillespie. A rigorous derivation of the chemical master equation. *Physica A*, (188):404–425, 1992.

[19] D. Graham and D. McRuer. *Analysis of Nonlinear Control Systems*. Wiley, New York, 1961.

[20] J. Greenblatt, J. R. Nodwell, and S. W. Mason. Transcriptional antitermination. *Nature*, 364(6436):401–406, 1993.

[21] L.H. Hartwell, J.J. Hopfield, S. Leibler, and A.W. Murray. From molecular to modular cell biology. *Nature*, 402:47–52, 1999.

[22] R. Heinrich, B. G. Neel, and T. A. Rapoport. Mathematical models of protein kinase signal transduction. *Molecular Cell*, 9:957–970, 2002.

[23] C. F. Huang and J. E. Ferrell. Ultrasensitivity in the mitogen-activated proteinkinase cascade. *Proc. Natl. Acad. Sci.*, 93(19):10078–10083, 1996.

[24] B. Ingalls. A frequency domain approach to sensitivity analysis of biochemical networks. *Journal of Physical Chemistry B-Condensed Phase*, 108(3):143–152, 2004.

[25] F. Jacob and J. Monod. Genetic regulatory mechanisms in the synthesis of proteins. *J. Mol. Biol.*, 3:318–56, 1961.

[26] N. G. Van Kampen. *Stochastic Processes in Physics and Chemistry*. Elsevier, 1992.

[27] P. Kokotovic, H. K. Khalil, and J. O'Reilly. *Singular Perturbation Methods in Control*. SIAM, 1999.

[28] H. Madhani. *From a to alpha: Yeast as a Model for Cellular Differentiation*. CSHL Press, 2007.

[29] J. Mallet-Paret and H.L. Smith. The Poincaré-Bendixson theorem for monotone cyclic feedback systems. *J. of Dynamics and Differential Equations.*, 2:367–421, 1990.

[30] J. D. Murray. *Mathematical Biology,* Vols. I and II. Springer-Verlag, New York, 3rd edition, 2004.

[31] R. M. Murray. *Optimization-Based Control*. http://www.cds.caltech.edu/~murray/amwiki/OBC, Retrieved 20 December 2009.

[32] National Center for Biotechnology Information. A science primer. Retrieved 20 December 2009, 2004. http://www.ncbi.nlm.nih.gov/About/primer/genetics.html.

[33] National Human Genome Research Institute. Talking glossary of genetic terms. Retrieved 20 December 2009. http://www.genome.gov/glossary.

[34] R. Phillips, J. Kondev, and J. Theriot. *Physical Biology of the Cell*. Garland Science, 2008.

[35] M. Ptashne. *A genetic switch*. Blackwell Science, Inc., 1992.

[36] C. V. Rao, J. R. Kirby, and A. P. Arkin. Design and diversity in bacterial chemotaxis: A comparative study in escherichia coli and bacillus subtilis. *PLoS Biology*, 2(2):239–252, 2004.

[37] G. De Rubertis and S. W. Davies. A genetic circuit amplifier: Design and simulation. *IEEE Trans. on Nanobioscience*, 2(4):239–246, 2003.

[38] J. Saez-Rodriguez, A. Kremling, H. Conzelmann, K. Bettenbrock, and E. D. Gilles. Modular analysis of signal transduction networks. *IEEE Control Systems Magazine*, pages 35–52, 2004.

[39] J. Saez-Rodriguez, A. Kremling, and E.D. Gilles. Dissecting the puzzle of life: modularization of signal transduction networks. *Computers and Chemical Engineering*, 29:619–629, 2005.

[40] H. M. Sauro and B. Ingalls. MAPK cascades as feedback amplifiers. Technical report, http://arxiv.org/abs/0710.5195, Oct 2007.

[41] H. M. Sauro and B. N. Kholodenko. Quantitative analysis of signaling networks. *Progress in Biophysics & Molecular Biology*, 86:5–43, 2004.

[42] H.M. Sauro. The computational versatility of proteomic signaling networks. *Current Proteomics*, 1(1):67–81, 2004.

[43] M. A. Savageau. Biochemical systems analysis. i. some mathematical properties of the rate law for the component enzymatic reactions. *J. Theoretical Biology*, 25:365–369, 1969.

[44] D. L. Schilling and C. Belove. *Electronic Circuits: Discrete and Integrated*. McGraw Hill, 1968.

[45] S. S. Shen-Orr, R. Milo, S. Mangan, and U. Alon. Network motifs in the transcriptional regulation network of *Escherichia coli*. *Nat. Genet.*, 31(1):64–68, 2002.

[46] L. Villa-Komaroff, A. Efstratiadis, S. Broome, P. Lomedico, R. Tizard, S. P. Naber, W. L. Chick, and W. Gilbert. A bacterial clone synthesizing proinsulin. *Proc. Natl. Acad. Sci. U.S.A.*, 75(8):372731, 1978.